Temperature Sensitive Electrical Parameters Selection for 10 kV SiC Power Module

Min Lin[1], Ruirui Chen[1], Dingrui Li[1], Leon M. Tolbert[1], Fred Wang[1,2], Hua Bai[1]

[1]*CURENT, Min H. Kao Department of Electrical Engineering and Computer Science, The University of Tennessee,*
[2]*Oak Ridge National Laboratory*
Knoxville, TN, USA
mlin12@vols.utk.edu, rchen14@vols.utk.edu, dli35@vols.utk.edu, tolbert@utk.edu, fred.wang@utk.edu, hbai2@utk.edu

Abstract—**This paper presents temperature sensitive electrical parameters (TSEPs) selection for a 10 kV silicon carbide (SiC) MOSFET power module. Static parameters including ON-state resistance and threshold voltage are introduced. A double pulse test (DPT) platform is built to test the power module on a hotplate, and the switching transient behavior in a temperature range from 25℃ to 125℃ is analyzed in detail. Various parameters during turn on and turn off are measured and compared based on their temperature linearity and sensitivity. Load current and gate resistance impacts on measurement are discussed, as well as comparisons to low voltage SiC MOSFETs.**

Keywords—10kV SiC power module, TSEP, double pulse test

I. INTRODUCTION

Excessive heat and thermal cycling are a major cause for device degradation [1] and failure. Therefore, to protect switching devices from overheating, junction temperature monitoring is crucial in health management. One method to measure device junction temperature is to embed a negative temperature coefficient (NTC) resistor close to the die in the module package. However, direct temperature measurement is often inaccessible for most power modules.

TSEP is another popular method because it is easily measurable and offers fast response. It can monitor the device online with a certain level of precision. It does not affect the normal operation of the device, nor requires complex circuits. TSEP is widely discussed in 1200 V IGBT power modules [2] [3]. In [4], voltage overshoot on bus parasitic inductance due to turn off di/dt is measured to monitor the temperature. In [5], turn off di/dt is also used as a TSEP, where voltage overshoot on leakage inductance of the Kelvin source is measured. Unlike IGBTs, turn off di/dt is not temperature dependent for SiC MOSFET [6], thus other TSEPs are adopted instead.

On-state resistance is calculated in [7] for temperature estimation of a 1.2 kV SiC MOSFET, which uses a printed circuit board (PCB) embedded Rogowski coil for measuring drain-source current and a two diode circuit for measuring drain-source voltage. Turn off delay time is measured in [8], but a large gate resistance is used to increase its sensitivity which significantly increases the switching loss. Reference [9] offers a comparison between threshold voltage, on state resistance, and

switching transients of 1.2 kV SiC MOSFET from different manufacturers. TSEP of 3.3 kV SiC MOSFET are presented in [10], and its intrinsic material behaviors are explained by numerical expressions.

Few papers have discussed TSEP of 10 kV SiC devices. A model of 10 kV discrete device switching behavior under different temperature is presented in [11]. However, it does not identify a suitable TSEP for overheating protection or device health monitoring. Test results of 10 kV power modules are given in [12], [13]; they mostly focus on general performance, such as on state resistance, switching loss, and short circuit withstand time. In this paper, potential TSEPs of a 10 kV 100 A SiC MOSFET power module are presented based on static test and DPT results. Its temperature sensitivity and linearity are discussed in detail for future implementation.

The rest of the paper is organized as follows. Section II introduces TSEPs based on static characterization. Section III covers TSEPs based on switching behavior from DPT results. The impacting factors such as load current and gate resistance are presented in Section IV. Section V draws the conclusion.

TABLE I - PARAMETERS OF THE XHV-9 10 kV SiC

Static parameters	Wolfspeed XHV-9 SiC MOSFET Module
Minimum Breakdown voltage	10 kV @ V_{gs}= 0 V, I_d = 6 mA
ON state resistance	50 $m\Omega$@ V_{gs}= 15 V, I_d = 90 A, T_j = 25℃
Maximum junction temperature	175 ℃

MOSFET Module

II. STATIC CHARACTERISTICS

The power module investigated is a Wolfspeed XHV-9 10 kV SiC MOSFET half bridge module. Each device has six dies in parallel; the detailed specifications are given in Table I. Static tests are conducted using curve tracer Keysight B1505A to measure forward conduction, reverse conduction, and transfer characteristics. Junction capacitance which includes C_{gs}, C_{ds}

and C_{gd} values remain stable across a wide temperature range, so they are not normally considered for TSEPs.

A. Forward Conduction Characteristics

Curve tracer is used to exert controlled duration and magnitude of gate source and drain source voltage pulses to the power module. The forward conduction test is conducted by restraining V_{ds} to less than 25 V and i_{ds} to less than 110 A, V_{gs} is swept from 1 V to 15 V by 1 V steps. In this way, the full operation range of normal working condition is measured without exposing the power module to excessive power and current. The forward conduction curve at 25℃ is presented in Fig. 1. The same test is repeated under 25℃, 50℃, 75℃, 100℃ and 125℃ by placing the power module on a hotplate with controlled temperature.
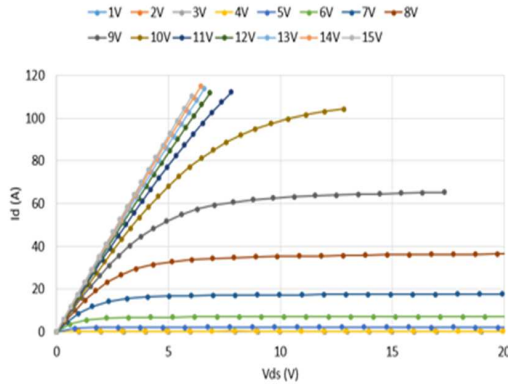

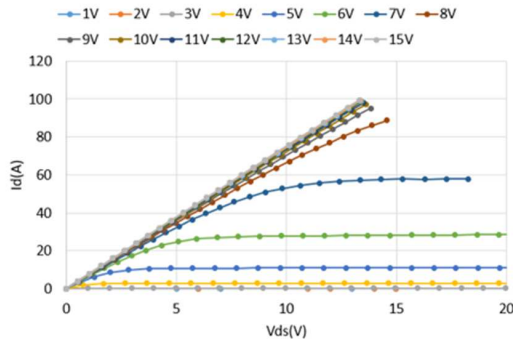Fig. 1. Forward conduction curve of the 10 kV SiC MOSFET module at 25℃.

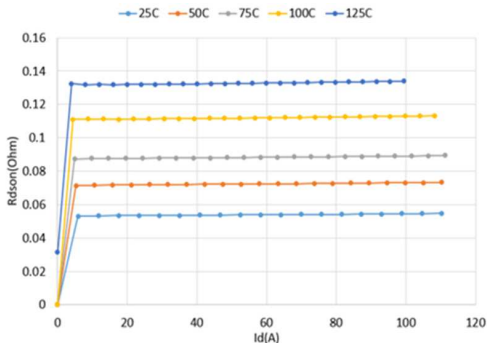Fig. 2. Forward conduction curve of the 10 kV SiC MOSFET module at 125℃.

Fig. 3. ON-resistance of the 10 kV SiC MOSFET module at different temperatures.

Based on the forward conduction curve, the ON-resistance at different temperatures when V_{gs} is 15 V are summarized in Fig. 3. It increases with higher temperature, but the increment is not uniform. Threshold voltage V_{th} can be extracted from the data. It decreases with increasing temperature because of the positive temperature dependence of the intrinsic carrier concentration. It is verified with measurement shown in Fig. 4.
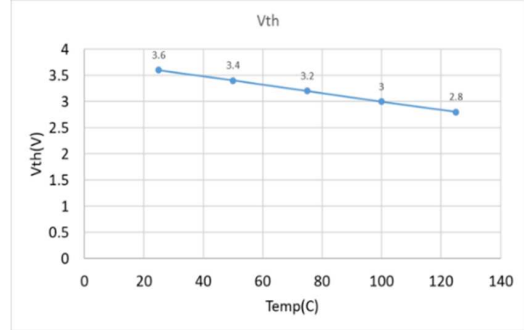

Fig. 4. Threshold voltage of the 10 kV SiC MOSFET module.

B. Reverse Conduction Characteristics

Reverse conduction curve is measured in a similar process of the forward conduction curve. V_{gs} is stepped from 1 V to 15 V with 2 V steps. V_{ds} is limited to -15 V and i_{ds} is restrained to -110 A. The reverse conduction curve at 25℃ is presented in

Fig. 5. Calculating R_{dson} for different temperatures as shown in
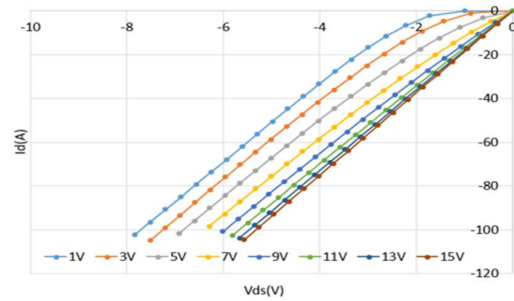
Fig. 6, it also increases with the temperature.
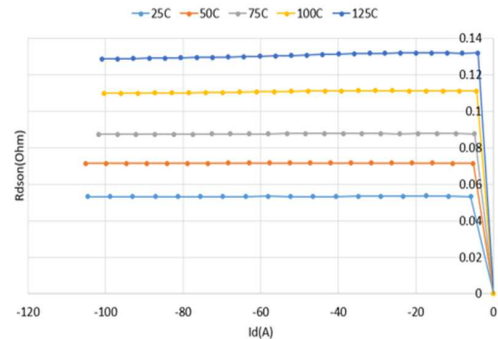

Fig. 5. Reverse conduction curve at 25℃.

Fig. 6. Reverse ON-resistance at different temperatures.

C. Transfer Characteristics

In Fig. 7, i_d is measured when $V_{ds} = 10$ V and V_{gs} is stepped from 1 V to 15 V. Transconductance is calculated in Fig. 8; it increases with the temperature when current is less than 40

5526

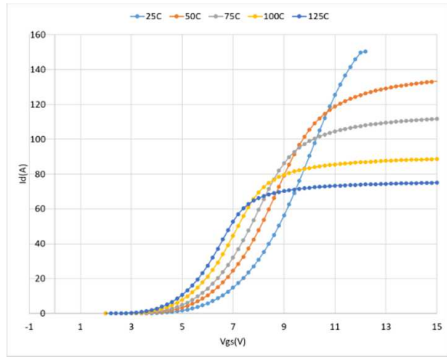A. When current is larger than 40 A, it does not change linearly with the temperature.

Fig. 7. Transfer characteristics of the 10 kV SiC MOSFET module at different temperatures.
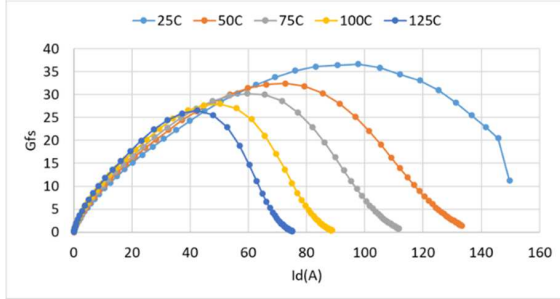

Fig. 8. Transconductance of the 10 kV SiC MOSFET module at different temperatures.

III. SWITCHING TRANSIENT CHARACTERISITICS

A. Experimental Test Setup

The DPT platform as shown in Fig. 10 was built to test 10 kV half bridge power module switching characteristics [14]. The key components are described as follows. The dc link capacitor consists of four 2 kV 360 uF capacitors in series connection. The dc link voltage can be adjusted from 0 to 7 kV. Due to the parasitic inductance in the commutation loop, a decoupling capacitor board is used to limit the voltage overshoot. The load inductance is 5 mH.

A circuit breaker with three Si IGBTs in series is connected in the main circuit to limit the maximum current in case a short circuit happens during testing. The dedicated gate driver receives control signals and transmits feedback signal by optical fiber, connecting to the controller outside of the high voltage room. This provides high voltage isolation, ensures signal integrity, and personnel safety. The gate driver has desat protection integrated, which protects the power module from short circuit faults. Gate turn on voltage is 15 V and turn off voltage is -5V. Gate resistance is 5 Ω. The auxiliary power supply that provides power to the gate driver has a 10 kV isolation and 2 pF coupling capacitance [15].

The measurement probes with sufficient bandwidth and isolation are used. Drain source voltage is measured by high voltage differential probe DP20-10k (17.5 kV, 120 MHz). Device current is measured by PEM CWTMIni50HF Rogowski coil (50 MHz). Gate source voltage is measured by TPP1000 Tektronix passive voltage probe (1 GHz).
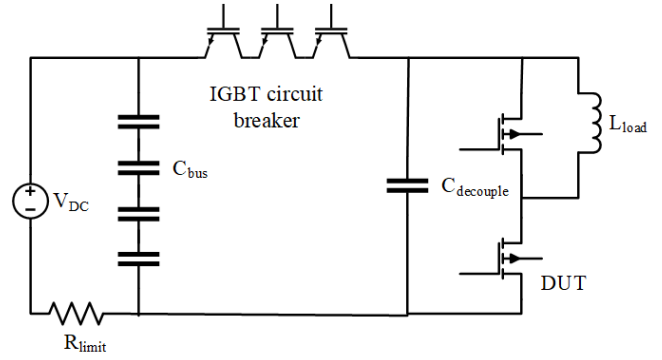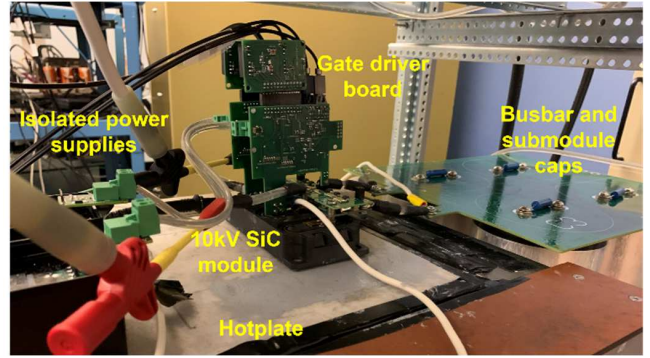

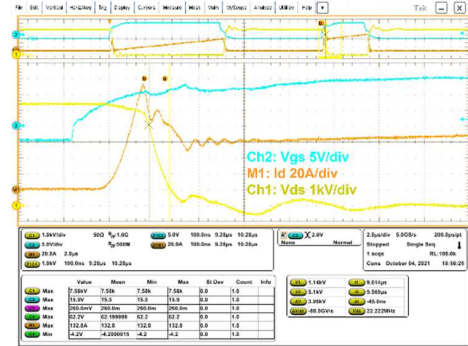Fig. 9. DPT circuit scheme .

Fig. 10. DPT experiment setup.

Fig. 11. Turn on switching transient at 6.5 kV 57 A.

B. Turn on Transient TSEP

TSEP during the switching process is divided into two groups, TSEP during the turn on transient, and TSEP during the turn off transient. Normally, turn on delay time, current rise rate, and drain source voltage drop time are temperature dependent. These data can be extracted from DPT results. Fig. 11 shows a typical turn on waveform conducted at 6.5 kV 57 A.

1) Turn-on Delay Time

During turn on delay time, the device is in cutoff region, C_{gs} charges from 0 V to V_{th}. Turn on delay time t_{don} in (1) measures the time when i_d starts to conduct after gate source voltage is applied to the device. Here, V_{cc} is turn on gate voltage, and V_{ee} is turn off gate voltage. R_g is gate resistance

and C_{iss} is input capacitance of power module. From previous analysis, threshold voltage drops with increasing temperature, t_{don} decreases as it takes shorter time for C_{gs} to charge to V_{th}.

$$t_{don} = R_g C_{iss} \ln\left(\frac{V_{cc} - V_{ee}}{V_{cc} - V_{th}}\right) \quad (1)$$

2) Current Rise Time

As soon as gate source voltage reaches V_{th}, the device starts conducting. The current rise time t_{ir} can be derived from (2), where I_L is load current and g_m is transconductance.

$$t_{ir} = R_g C_{iss} \ln\left[\frac{V_{cc} - V_{th}}{V_{cc} - V_{th} - \frac{I_L}{g_m}}\right] \quad (2)$$

3) Voltage Fall Time

Drain source voltage starts to fall from nonconducting high voltage the moment V_{gs} reaches miller plateau and C_{gd} starts discharging. Thus, drain source voltage fall time t_{vf} is given in (3), where Q_{gd} is gate charge.

$$t_{vf} = \frac{R_g Q_{gd}}{V_{cc} - V_{th} - \frac{I_L}{g_m}} \quad (3)$$

V_{th} has a negative temperature coefficient. g_m is also affected by temperature, but in this case and unlike the value measured by the curve tracer where drain source voltage equals 10 V, the actual drain source voltage is several kilovolts during switching transient of DPT. Transconductance varies with drain source voltage from 20 V to 7 kV in [16], but its temperature dependency is unknown. Thus, it is difficult to estimate the above parameters' relation with temperature based on equation only. From test results in Fig. 12, t_{don}, t_{cr} and t_{vf} drops linearly with increasing temperature.
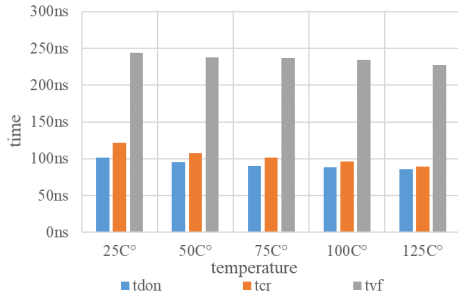

Fig. 12. t_{don}, t_{cr}, t_{vf} decreases with increasing temperature.

C. Turn off transient TSEP

1) Turn-off Delay Time

Turn-off delay time t_{doff} measures the time from the instant when gate-source voltage drops to the instant when drain-source voltage starts to increase from zero.

$$t_{doff} = R_g C_{iss} \ln\frac{V_{cc} - V_{ee}}{V_{th} + \frac{I_L}{g_m} - V_{ee}} \quad (4)$$

As threshold voltage is negatively correlated with temperature, and transconductance is nonlinearly dependent on temperature, it is difficult to derive from equation alone the relation between turn off delay time and the temperature. From

the experiment results in Fig. 13, when $R_g = 5\ \Omega$, turn off delay time has a small variance of less than 5% across the whole temperature range when current is between 16.6 A to 47.8 A. At 7.1 A and 56.9 A, it changes nonlinearly with temperature.
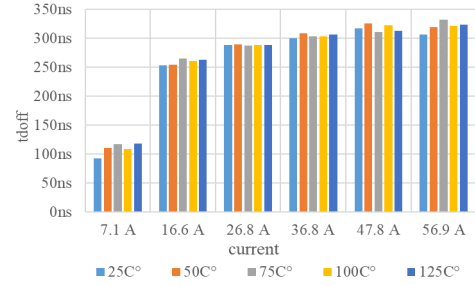

Fig. 13. Turn off delay time at $R_g = 5\ \Omega$ is similar at different temperatures.

However, when $R_g = 2\ \Omega$, it increases linearly with increasing temperature in Fig. 14. The values at 7.1 A are significantly smaller than measurements at higher current, and do not follow the general trend.
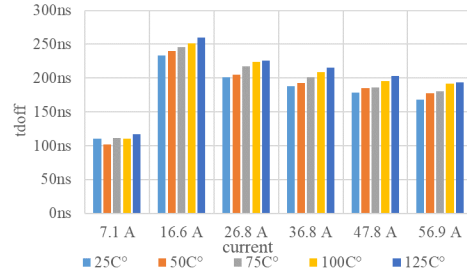

Fig. 14. Turn off delay time at $R_g = 2\ \Omega$.

2) Voltage Rise Time

The turn-off transient of this 10 kV SiC power module is dominated by load current charging/discharging the device junction capacitances. As the device capacitance is temperature independent, most parameters are not affected by temperature. The voltage rise time has stable duration regardless of the temperature change. In Fig. 15, voltage rise time difference across full temperature range from 25℃ to 125℃ is less than 4% when load current is less than 20 A. When load current is larger than 20 A, it is less than 5 ns. Voltage slew rate dv/dt corresponds with voltage rise time and is also temperature insensitive.

The same phenomenon is also observed in voltage overshoot V_{os} as shown in Fig. 16. It does not show a clear relation to the temperature. From above results, for this 10 kV SiC MOSFET module, only the turn-off delay time at considerable fast switching speed condition, i.e., with small gate resistance (<=2Ω) and considerable load current (>= 10 A), can be a suitable TSEP. Other parameters during turn off are not temperature sensitive or do not follow a linear trend.
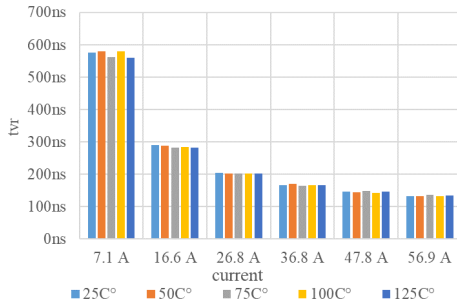
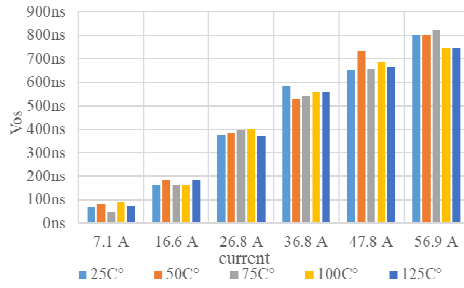Fig. 15. t_{vr} is stable across whole temperature range.

Fig. 16. Voltage overshoot at different temperatures.

IV. IMPACTING FACTORS

This section discusses other factors besides temperature that impact the electrical parameters measured, especially during switching transients. Gate turn on voltage and turn off voltage affect the switching speed and can be controlled in a versatile way with an intelligent gate driver. In this application, the power module is switched on and off by 15 V and -5 V respectively, so gate voltage impact is not investigated.

A. Gate Resistance

It is straightforward that gate resistance has a positive impact on t_{don}, t_{ir}, and t_{vf} as shown in (1)-(4) .Thus, gate resistance can be used to increase temperature sensitivity of these TSEP, so it has a larger variance over same temperature range. It is verified by the test results in Table III where $R_g = 5\,\Omega$ and is higher than those measured in Table II where $R_g = 2\,\Omega$.

TABLE II. TURN ON RESULTS AT 2 Ω

Temperature	t_{don} (ns)	t_{cr}(ns)	t_{vf} (ns)
25 C°	67.6	58	200.8
50 C°	66.5	57	198.8
75 C°	63	54.4	199.6
100 C°	62	51	191.6
125 C°	61	47.8	191.6

TABLE III. TURN ON RESULTS AT 5 Ω

Temperature	t_{don} (ns)	t_{cr}(ns)	t_{vf} (ns)
25 C°	101.6	121.6	244.4
50 C°	95.4	107.4	238.2
75 C°	90.6	101.8	236.6
100 C°	88.4	96	234.6
125 C°	86	89	227.6

B. Load Current

The following data are extracted from DPT waveforms at the same dc voltage 6.4 kV with varying current. During the turn on process, load current does not affect turn on delay time from theoretical analysis in (4). It is verified through test results in Fig. 17, where at the same temperature turn on delay time shows a small variance of less than 10 ns as current increases from 7.1 A to 56.9 A. By contrast, current rise time increases as shown in

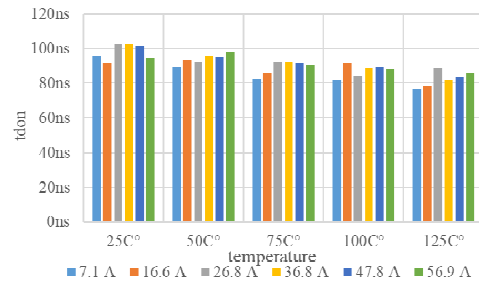Fig. 18, while voltage fall time decreases in Fig. 19 with increasing load current.

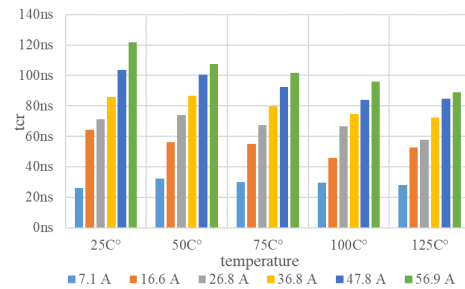Fig. 17. t_{don} measured at different currents and temperatures.

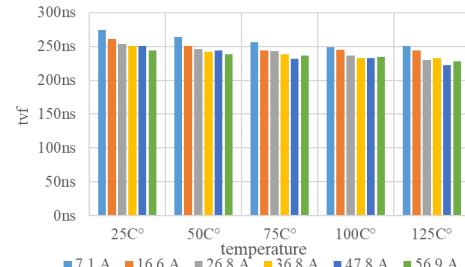Fig. 18. t_{cr} increases with larger current.

Fig. 19. t_{vf} decreases with higher current.

5529

TABLE IV. TSEP TEMPERATURE SENSITIVITY

TSEP	TSEP Symbols	Temperature Coefficient
Threshold voltage	V_{th}	-0.08 V/℃
Turn on delay time	t_{don}	-106 ps/℃
Current rise time	t_{cr}	-306 ps/℃
Voltage fall time	t_{vf}	-149 ps/℃

V. CONCLUSION

In this paper, TSEP for the Wolfspeed XHV-9 10 kV SiC MOSFET power module is investigated. On state resistance and threshold voltage can be extracted as TSEP. Threshold voltage shows better temperature linearity. Turn on TSEPs include turn on delay time, current rise time and voltage fall time, which all have negative temperature coefficients. Only turn on delay time is not affected by load current, while the other two have to be calibrated with current. Their temperature sensitivity can be improved by increasing the gate resistance. Turn off TSEP only has one candidate which is turn off delay time. Voltage rise time and voltage overshoot are not temperature sensitive.

The temperature sensitivity is summarized in Table IV when gate resistance is 5 ohm. Compared with low voltage 3.3 kV, 5 A SiC MOSFET in [10], 10 kV SiC MOSFET power module have the same TSEP of turn on delay time, current rise time and turn off delay time. Turn on current switching rate, which is calculated from current rise time, for a 10 kV, 100 A SiC MOSFET is 1600 A/(ms·℃) , compared with 328 A/(ms·℃) for a 3.3 kV SiC MOSFET. Turn on delay time is also significantly larger in 10 kV device than -18.6 ps/℃ of 3.3 kV device. Threshold voltage temperature sensitivity is also higher than 1.2 kV 30A devices at -0.005 V/℃ in [9]. Due to limited data available for SiC MOSFET, only a number of TSEPs can be compared. Unlike 3.3 kV and 1.2 kV devices, voltage slew rate dv/dt, voltage overshoot and switching loss during turn off cannot be selected as TSEP.

ACKNOWLEDGMENT

REFERENCES

[1] H. Luo, F. Iannuzzo, F. Blaabjerg, M. Turnaturi, and E. Mattiuzzo, "Aging precursors and degradation effects of SiC-MOSFET modules under highly accelerated power cycling conditions," in *2017 IEEE Energy Conversion Congress and Exposition (ECCE)*, Oct. 2017, pp. 2506–2511.

[2] Y. Yang and P. Zhang, "*In Situ* insulated gate bipolar transistor junction temperature estimation method via a bond wire degradation independent parameter turn-off *Vce* overshoot," *IEEE Trans. Ind. Electron*, vol. 68, no. 10, pp. 10118–10129, Oct. 2021.

[3] U.-M. Choi, F. Blaabjerg, S. Jørgensen, S. Munk-Nielsen, and B. Rannestad, "Reliability improvement of power converters by means of condition monitoring of IGBT modules," *IEEE Trans. Power Electron*, vol. 32, no. 10, pp. 7990–7997, Oct. 2017.

[4] Y. Yang and P. Zhang, "A novel converter-level IGBT junction temperature estimation method based on the bus voltage ringing," *IEEE Trans. Power Electron*, vol. 37, no. 4, pp. 4553–4563, Apr. 2022.

[5] Y. Chen *et al.*, "A thermo-sensitive electrical parameter with maximum dIC/dt during turn-off for high power trench/field-stop IGBT modules," in *2016 IEEE Applied Power Electronics Conference and Exposition (APEC)*, Long Beach, CA, USA, Mar. 2016, pp. 499–504.

[6] A. Griffo, J. Wang, K. Colombage, and T. Kamel, "Real-time measurement of temperature sensitive electrical parameters in SiC power MOSFETs," *IEEE Trans. Ind. Electron*, vol. 65, no. 3, pp. 2663–2671, Mar. 2018.

[7] S. Mocevic, V. Mitrovic, J. Wang, R. Burgos, and D. Boroyevich, "Gate-driver integrated junction temperature estimation of SiC MOSFET modules," *IEEE J. Emerg. Sel. Top. Power Electro.*, vol. 10, no. 5, pp. 4965–4980, Oct. 2022.

[8] L. Qiao, F. Wang, J. Dyer, and Z. Zhang, "Online junction temperature monitoring for SiC MOSFETs using turn-on delay time," in *2020 IEEE Applied Power Electronics Conference and Exposition (APEC)*, New Orleans, LA, USA, Mar. 2020.

[9] C. DiMarino, Z. Chen, M. Danilovic, D. Boroyevich, R. Burgos, and P. Mattavelli, "High-temperature characterization and comparison of 1.2 kV SiC power MOSFETs," in *2013 IEEE Energy Conversion Congress and Exposition*, Denver, CO, USA, Sep. 2013.

[10] Z. Ni, S. Zheng, M. S. Chinthavali, and D. Cao, "Investigation of dynamic temperature-sensitive electrical parameters for medium-voltage SiC and Si devices," *IEEE J. Emerg. Sel. Top. Power Electron*, vol. 9, no. 5, pp. 6408–6423, Oct. 2021.

[11] S. Ji, S. Zheng, F. Wang, and L. M. Tolbert, "Temperature-dependent characterization, modeling, and switching speed-limitation analysis of third-generation 10-kV SiC MOSFET," *IEEE Trans. Power Electron*, vol. 33, no. 5, pp. 4317–4327, May 2018.

[12] D. Johannesson, M. Nawaz, and K. Ilves, "Assessment of 10 kV, 100 A silicon carbide MOSFET power modules," *IEEE Trans. Power Electron*, vol. 33, no. 6, pp. 5215–5225, Jun. 2018.

[13] A. N. Lemmon and R. C. Graves, "Comprehensive characterization of 10-kv Silicon Carbide half-bridge modules," *IEEE J. Emerg. Sel. Top. Power Electron.*, vol. 4, no. 4, pp. 1462–1473, Dec. 2016.

[14] H. Li, Z. Gao, R. Chen, and F. Wang, "Improved double pulse test for accurate dynamic characterization of medium voltage SiC devices," *IEEE Trans. Power Electron.*, vol. 38, no. 2, pp. 1779-1790, Sep. 2022.

[15] L. Zhang *et al.*, "Design considerations for high-voltage insulated gate drive power supply for 10-kV SiC MOSFET applied in medium-voltage converter," *IEEE Trans. Ind. Electron.*, vol. 68, no. 7, pp. 5712–5724, Jul. 2021.

[16] R. Chen, M. Lin, X. Huang, F. Wang, and L. M. Tolbert, "An improved turn-on switching transient model of 10 kV SiC MOSFET," in *2022 IEEE Applied Power Electronics Conference and Exposition (APEC)*, Mar. 2022, pp. 1–8.